Acta Pharmacologica Sinica (2012) 33: 941–952
 1671-4083/12 $32.00
www.nature.com/aps

Original Article

Arctigenin alleviates ER stress via activating AMPK

Yuan GU[1], Xiao-xiao SUN[1], Ji-ming YE[2], Li HE[1], Shou-sheng YAN[1], Hao-hao ZHANG[1], Li-hong HU[3], Jun-ying YUAN[4], Qiang YU[1, *]

[1]Department of Tumor Pharmacology, and [3]State Key Laboratory of Drug Research, Shanghai Institute of Materia Medica, Chinese Academy of Sciences, Shanghai 201203, China; [2]Health Innovations Research Institute and School of Health Sciences, RMIT University, Melbourne, Australia; [4]Department of Cell Biology, Harvard Medical School, Boston, USA

Aim: To investigate the protective effects of arctigenin (ATG), a phenylpropanoid dibenzylbutyrolactone lignan from *Arctium lappa* L (Compositae), against ER stress *in vitro* and the underlying mechanisms.
Methods: A cell-based screening assay for ER stress regulators was established. Cell viability was measured using MTT assay. PCR and Western blotting were used to analyze gene and protein expression. Silencing of the CaMKKβ, LKB1, and AMPKα1 genes was achieved by RNA interference (RNAi). An ATP bioluminescent assay kit was employed to measure the intracellular ATP levels.
Results: ATG (2.5, 5, and 10 μmol/L) inhibited cell death and unfolded protein response (UPR) in a concentration-dependent manner in cells treated with the ER stress inducer brefeldin A (100 nmol/L). ATG (1, 5, and 10 μmol/L) significantly attenuated protein synthesis in cells through inhibiting mTOR-p70S6K signaling and eEF2 activity, which were partially reversed by silencing AMPKα1 with RNAi. ATG (1–50 μmol/L) reduced intracellular ATP level and activated AMPK through inhibiting complex I-mediated respiration. Pretreatment of cells with the AMPK inhibitor compound C (25 μmol/L) rescued the inhibitory effects of ATG on ER stress. Furthermore, ATG (2.5 and 5 μmol/L) efficiently activated AMPK and reduced the ER stress and cell death induced by palmitate (2 mmol/L) in INS-1 β cells.
Conclusion: ATG is an effective ER stress alleviator, which protects cells against ER stress through activating AMPK, thus attenuating protein translation and reducing ER load.

Keywords: arctigenin; ER stress; human hepatocellular liver carcinoma cell; β-cell death; mTOR-p70S6K; eukaryotic translation elongation factor 2 (eEF2); mitochondrial respiration; AMPK

Acta Pharmacologica Sinica (2012) 33: 941–952; doi: 10.1038/aps.2012.60; published online 18 Jun 2012

Introduction

The endoplasmic reticulum (ER) is a highly dynamic organelle in which proteins and lipids are synthesized, modified, and transported. Under conditions such as glucose starvation, hypoxia, aberrant Ca^{2+} regulation, and virus infection, collectively known as ER stress, proteins fail to be correctly folded and eventually accumulate and aggregate in the ER lumen. In response to the abnormalities in the ER, the ER stress response or the unfolded protein response (UPR) is triggered by three ER-localized transmembrane proteins: PKR-like ER kinase (PERK), activation transcription factor (ATF6), and inositol-requiring kinase (IRE1). During the ER stress response, PERK phosphorylates and inhibits eukaryotic initiation factor 2α (eIF2α), leading to translation attenuation[1]; ATF6 translocates to the Golgi, where it is sequentially cleaved by the S1P and S2P proteases to form an active 50 kDa transcription factor[2]; and IRE1 cleaves the mRNA transcript of X box protein 1 (XBP1) by an unconventional splicing mechanism[3]. The activation of these pathways restricts protein load on the ER through transient attenuation of general protein synthesis, promotes degradation of misfolded proteins and increases protein folding capacity in the ER[4]. However, severe or prolonged accumulation of unfolded proteins triggers apoptosis of target cells.

Accumulating evidence suggest that ER stress is implicated in a wide range of diseases, including diabetes, neurodegeneration, stroke, cardiac disease, muscle degeneration and others[5]. Particularly, ER stress has been reported to play a central role in pancreatic β-cell demise in type 2 diabetes and perhaps also in type 1 diabetes[6]. Elevated ER stress markers have been detected in islet tissues of diet-induced and genetic *db/db* diabetic mice[7], as well as of type 2 diabetes patients[8]. Thus, we hypothesize that alleviation of ER stress may represent an attractive therapeutic strategy for the treatment of

* To whom correspondence should be addressed.
E-mail qyu@sibs.ac.cn
Received 2012-02-28 Accepted 2012-05-02

β-cell death in type 2 diabetes.

Arctigenin (ATG) is a phenylpropanoid dibenzylbutyrolactone lignan from *Arctium lappa* L (Compositae)[9]. *Arctium lappa* L, commonly known as burdock, has been widely used in traditional Chinese medicine (TCM) for treating inflammation[10]. It has also been used therapeutically in Europe and North America for hundreds of years[11]. The root of *Arctium lappa* L, a popular edible vegetable in China and Japan, is used to make a general health tonic. Previous studies have shown that ATG exerted protective effects against oxidation[12], viral infection[13], and cancer[14]. Most recently, two research groups have reported that ATG could block the UPR and preferentially inhibit tumor cell viability under glucose-deprived conditions[15, 16]. The molecular targets and mechanisms of ATG however remain unclear.

In the present study, we established a cell-based screening assay for ER stress regulators and identified ATG as a protective agent against ER stress, which efficiently protected HepG2 cells from the ER stress inducer brefeldin A (BFA)-induced cell death, and investigated its action mechanism. We then explored its therapeutic potential in treating diabetes by examining its effects on palmitate-induced β-cell death.

Materials and methods

Reagents and antibodies

Arctigenin (purity >99%), isolated from dried seeds of *A. lappa* as previously described[17], was provided by Dr Li-hong HU. Penicillin, streptomycin, Brefeldin A, compound C, 5-aminoimidazole-4-carboxamide ribonucleoside (AICAR), *D*-glucose, 3-(4,5-dimethylthiazol-2-yl)-2,5-diphenyltetrazolium bromide (MTT) and propidium iodide (PI) were purchased from Sigma (St Louis, Mo, USA). Palmitate was purchased from Takeda Chemical Industries (TCI, Tokyo, Japan). Fatty acid-free bovine serum albumin (BSA) was purchased from Equitech-Bio (Kerrville, TX, USA). α-MEM medium, RPMI-1640 medium and fetal bovine serum (FBS) were purchased from Invitrogen (Carlsbad, CA, USA). All other chemicals (molecular biology grade) were obtained from standard commercial sources. Anti-PARP antibody, anti-phosphorylated AMPKα (Thr172), anti-phosphorylated acetyl-CoA carboxylase (ACC, Ser79), anti-phosphorylated eIF2α (Ser51), anti-eIF2α, anti-phosphorylated mTOR (Ser2448), anti-mTOR, anti-phosphorylated p70S6K (Thr389), anti-p70S6K, anti-phosphorylated eEF2 (Thr56), anti-eEF2, and anti-GAPDH antibodies were purchased from Cell Signaling Technology (Beverly, MA, USA). Anti-AMPKα antibody was purchased from Epitomics (Burlingame, CA, USA).

Cell culture

HepG2 cells, a human hepatocellular liver carcinoma cell line, were grown in α-MEM containing 10% (*v/v*) FBS, 100 U/mL penicillin and 100 μg/mL streptomycin. INS-1 β-cells, a rat insulinoma cell line, were grown in RPMI-1640 medium supplemented with 10% FBS, 1 mmol/L sodium pyruvate, 2 mmol/L *L*-glutamine, 10 mmol/L HEPES, 0.05 mmol/L 2-mercaptoethanol, 100 units/mL penicillin and 100 mg/mL streptomycin. All cell lines were cultured at 37 °C in a humidified atmosphere of 95% air and 5% CO_2.

MTT assay and PI staining

Cell growth rate was measured by the MTT assay. Briefly, after treatment, 20 μL MTT (5 mg/mL) was added to the culture medium. After incubating for 3 h at 37 °C, the cells were solubilized in dimethyl sulfoxide (DMSO), and the absorbance of each well was measured at 570 nm with a spectrophotometer (Molecular Devices, Silicon Valley, CA, USA). Cell death was examined by PI staining. After treatment, cells were stained with 15 μg/mL PI for 10 min, and then washed with PBS and photographed using a UV microscope.

Western blot analysis

Cells were lysed with 1×Laemmli buffer (Sigma, St Louis, MO, USA) containing 2 mmol/L NaF and 2 mmol/L Na_3VO_4, which are used to prevent the dephosphorylation of serine/threonine and tyrosine residues, respectively. Proteins were separated by sodium dodecyl sulphate (SDS) polyacrylamide gel electrophoresis and transferred to a nitrocellulose membrane (Millipore, Bedford, MA, USA). Membrane was blocked in 5% nonfat milk for 1 h at room temperature and then subjected to immunostaining with primary antibodies at 4 °C overnight and peroxidase-conjugated secondary antibodies at room temperature for 1 h. Immunoreactivity was revealed with the Supersignal chemiluminescence dection kit (Pierce, Rockford, IL, USA). Immunoblots were scanned and quantified using the software ImageJ (NIH).

Isolation of total RNA, semiquantitative and quantitative reverse transcription PCR

Total RNA was extracted from cells using TRIzol reagent (Invitrogen, Paisley, UK) following the manufacturer's instructions. 4 μg total RNA and ReverTra Ace reverse transcriptase (Toyobo, Osaka, Japan) were used in the reverse transcription reaction.

Taq DNA polymerase (Takara, Tokyo, Japan) was used for the subsequent polymerase chain reaction (PCR). The specific primers for semiquantitative PCR were as follows: 5′-CCTTGTAGTTGAGAACCA-3′ (forward) and 5′-GGGCTTGGTATATATGTGGG-3′ (reverse) for both unspliced and spliced XBP-1 (human); 5′-ACCACAGTCCATGCCATCAC-3′ (forward) and 5′-TCCACCACCCTGTTGCTG-3′ (reverse) for GAPDH (human); 5′-TTACGAGAGAAAACTCATGGGC-3′ (forward) and 5′-GGGTCCAACTTGTCCAGAATGC-3′ (reverse) for both unspliced and spliced XBP-1 (rat); 5′-CCCCAATGTATCCGTTGTGGA-3′ (forward) and 5′-GCCTGCTTCACCACCTTCTT-3′ (reverse) for GAPDH (rat). RT–PCR for XBP-1 was performed for 30 cycles and GAPDH for 20 cycles. PCR products were separated on 8% polyacrylamide gel and visualized by ethidium bromide staining.

Quantitative PCR was performed and analyzed in ABI-PRISM 7700 Sequence Detection System (Applied Biosystems) with SYBR green real-time PCR kit (Takara).

The specific primer sequences were as follows: 5′-GGCCAGTTTGGTGTCGGTTT-3′ (forward) and 5′-CGTTCCCCGTCCTAGAGTGTT-3′ (reverse) for Grp94 (human); 5′-TGGACTGCAGGTGCTGATAG-3′ (forward) and 5′-GGATTCTTGGTTGCCTGGTA-3′ (reverse) for EDEM (human); 5′-TCAAACCTCATGGGTTCTCC-3′ (forward) and 5′-GTGTCATCCAACGTGGTCAG-3′ (reverse) for ATF4 (human); 5′-TGTGACCTCTGCTGGTTCTG-3′ (forward) and 5′-TGGAAGCCTGGTATGAGGAC-3′ (reverse) for CHOP (human); 5′- CACGTCCAACCCGGAGAA-3′ (forward) and 5′-ATTCCAAGTGCGTCCGATG-3′ (reverse) for Grp78 (Rat); 5′-TACTATGCCAGTCAGAAGAAAACG-3′ (forward) and 5′-CATCCTTTCTATCCTGTCTCCATA-3′ (reverse) for Grp94 (Rat); 5′-GACATGCCGCCTGGAGAAAC-3′ (forward) and 5′-AGCCCAGGATGCCCTTTAGT-3′ (reverse) for GAPDH (Rat).

RNA interference and transfection

Small interfering RNAs (siRNAs) against Ca^{2+}/calmodulin-dependent protein kinase kinase β (CaMKKβ), liver kinase B1 (LKB1) and AMPKα1 as well as a nonsilencing control siRNA were purchased from GenePhama (Shanghai, China). The siRNA sequences applied to target CaMKKβ were: 5′-CGAUCGUCAUCUCUGGUUAdTdT-3′ (sense) and 5′-UAACCAGAGAUGACGAUCGdTdT-3′ (antisense); for LKB1, 5′-GGCUCUUACGGCAAGGUGAdTdT-3′ (sense) and 5′-UCACCUUGCCGUAAGAGCCdTdT-3′ (antisense) and, for AMPKα1, 5′-UGCCUACCAUCUCAUAAUAdTdT-3′ (sense) and 5′-UAUUAUGAGAUGGUAGGCAdTdT-3′ (antisense) were used. The siRNA sequences employed as a negative control were 5′-UUCUCCGAACGUGUCACGUTT-3′ (sense) and 5′-ACGUGACACGUUCGGAGAATT-3′ (antisense).

Transfections of HepG2 cells with siRNA or a plasmid encoding green fluorescent protein were performed using Lipofectamine 2000 (Invitrogen) according to the manufacturer's protocol.

Determination of intracellular ATP content

The luciferin-luciferase assay was used to measure intracellular ATP levels. Briefly, after rinsing three times with PBS, cells were solubilized in 200 μL (for 24-well plate) of somatic cell ATP-releasing agent (Sigma, St Louis, MO, USA). Samples were centrifuged for 5 min in a microcentrifuge. Determination of ATP levels was accomplished by combining equal volumes of supernatant with an ATP assay mix (Sigma, St Louis, MO, USA) and measuring the level of chemiluminescence. Measurements are expressed as a percent of the initial value after subtraction of background countings.

Mitochondrial respiration measurements

Mitochondria were isolated from the muscles of male Wistar rats following standard procedures[18]. To measure respiration rate, mitochondria were incubated at 37 °C in a Clark type oxygen electrode (Strathkelvin Instruments, Motherwell, Scotland) in a buffer (pH 7.0) composed of 225 mmol/L mannitol, 75 mmol/L sucrose, 10 mmol/L Tris-HCl, 10 mmol/L KH_2PO_4, 10 mmol/L KCl, 0.8 mmol/L $MgCl_2$, 0.1 mmol/L EDTA, 0.3% fatty acid free BSA. The respiratory control ratio, the ratio of state III to state IV respiration, was approximately 5, indicating that the isolated mitochondria were well coupled. Effects of ATG on mitochondrial respiration were determined in the presence of excess ADP (2.4 mmol/L), using substrate combinations targeting either complex I (5 mmol/L pyruvate plus 2 mmol/L malate) or complex II (10 mmol/L succinate plus 4 μmol/L rotenone) of the respiratory chain.

Palmitate-BSA solution preparation

Palmitate was dissolved in ethanol: H_2O (1: 1, *v/v*) at 50 °C at a concentration of 400 mmol/L. The palmitate solution 150 μL was then mixed with 3 mL fatty acid-free BSA (20% solution in H_2O) by stirring at 37 °C for 1 h. The final molar ratio of palmitate to BSA was 6.7: 1 and the final concentration of palmitate-BSA is 20 mmol/L. All control conditions included a solution of vehicle (ethanol: H_2O) mixed with fatty acid-free BSA at the same concentration as the palmitate-BSA solution.

Statistical analysis

Triplicates were used in each experiment and data were shown only if three independent experiments showed consistent results. All results are expressed as the mean±SEM. Statistical differences between groups were determined by using the unpaired Student's *t*-test. $P<0.05$ was considered statistically significant. $P<0.05$, $P<0.01$ *vs* control.

Results

ATG protects HepG2 cells from BFA-induced apoptosis

We identified ATG as a protective agent against ER stress through a cell-based assay, in which ER stress was induced by treating HepG2 cells with BFA, an ER-to-Golgi vesicle transport inhibitor. The MTT assay demonstrated that only 27% of the cells had survived at 72 h after BFA treatment. However, ATG inhibited the BFA-induced cell death in a dose-dependent manner (Figure 1A). Meanwhile, a higher concentration of ATG (> 10 μmol/L) on its own caused a statistically significant decrease in cell number (Figure 1A), so we chose 5 μmol/L for further studies of its effects on reducing ER stress.

To determine whether ATG specifically affects the ER stress-induced cell death, we investigated the effects of ATG on cell death induced by non-ER stress stimuli, including protein synthesis inhibitor cycloheximide (CHX), DNA topoisomerase II inhibitor adriamycin (ADM), and the mitochondrial complex I inhibitor berberine (BBR)[18]. Our data showed that ATG had no protective effect against CHX-, ADM-, or BBR-induced cell death, which indicates that ATG may specifically inhibit ER stress-induced cell death (Figure 1B).

The protective effect of ATG against BFA-induced cell death was further confirmed by PI (propidium iodide) staining and PARP cleavage assay. As shown in Figure 1C, BFA increased the number of round and PI-stained cells, which were obviously inhibited by ATG. As reported, BFA induced apoptosis as indicated by poly (ADP-ribose) polymerase (PARP) cleavage. Co-treatment with ATG significantly prevented the BFA-

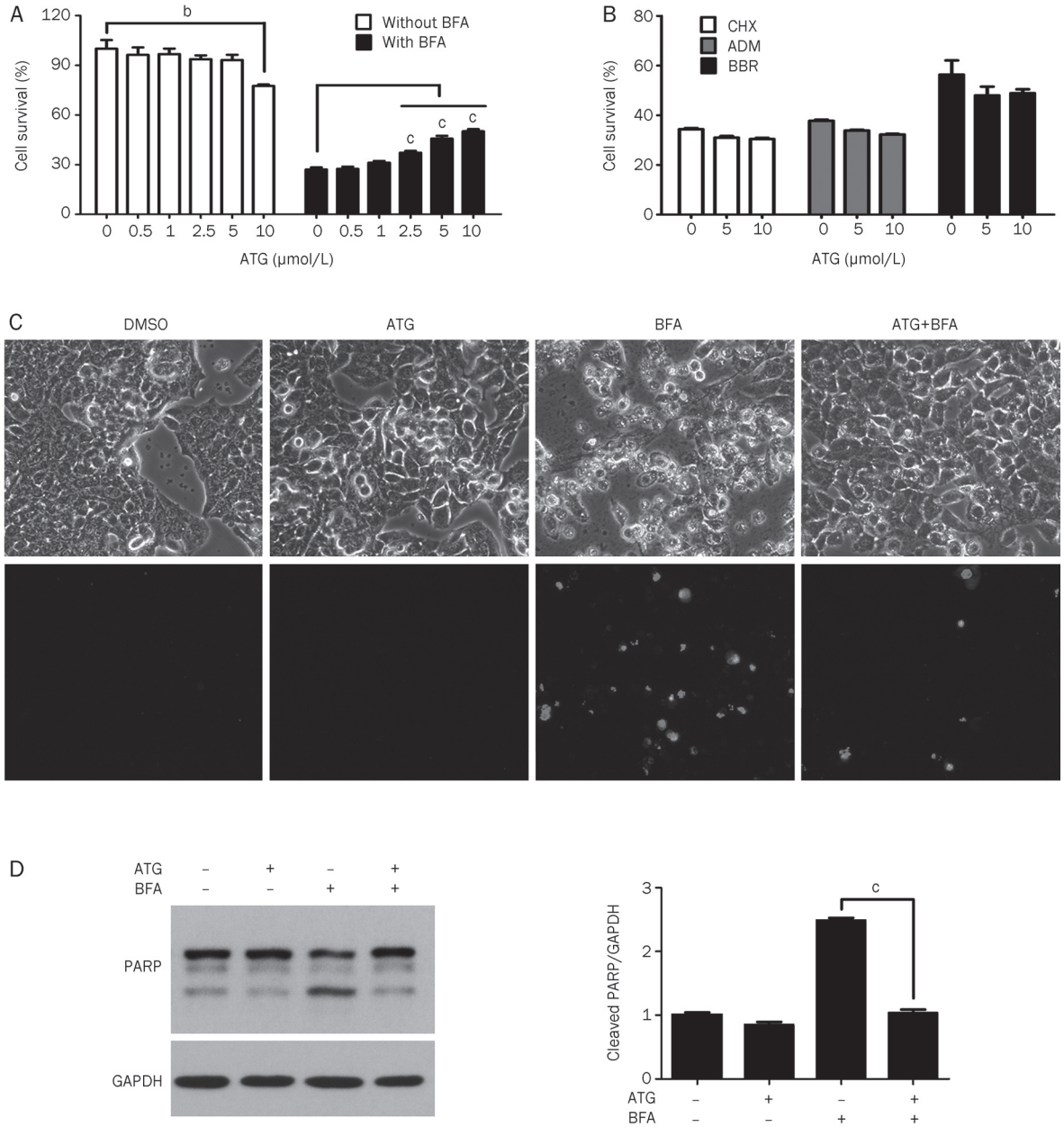

Figure 1. ATG specifically inhibits BFA-induced apoptosis. (A) HepG2 cells were cultured for 72 h with increasing concentrations of ATG alone, or in combination with 100 nmol/L BFA. Viable cell number was measured by MTT assay, and results were reported as a percentage relative to untreated cells. (B) HepG2 cells were cultured for 72 h with the indicated concentrations of ATG in the presence of CHX (50 μmol/L), ADM (500 nmol/L) or BBR (10 μmol/L). Cell growth rate was measured by MTT assay and results were reported as a percentage relative to untreated cells. (C) HepG2 cells were cultured for 48 h in the presence or absence of ATG (5 μmol/L) and/or BFA (100 nmol/L) followed by staining with PI (15 μg/mL) for 15 min. Representative images of cellular morphology (top panel) and PI staining (bottom panel) were shown at 200×magnification. (D) Cells were treated in the same way as in C. PARP cleavage was examined by Western blot analysis. Relative band intensity was normalized for GAPDH and expressed as a percentage compared with the value of untreated control. n=3 experiments. Mean±SEM. $^{b}P<0.05$, $^{c}P<0.01$ *vs* control.

induced PARP cleavage (Figure 1D). Meanwhile, ATG *per se* did not increase the number of PI-stained cells or induce PARP cleavage (Figure 1C and 1D). These data demonstrate that ATG can effectively protect HepG2 cells from the ER stress inducer (BFA)-induced apoptosis.

ATG down-regulates UPR signaling pathways induced by ER stress

To confirm that ATG protects cells from apoptosis by alleviating ER stress, we investigated the effects of ATG on UPR signaling pathways. Our data showed that BFA increased the

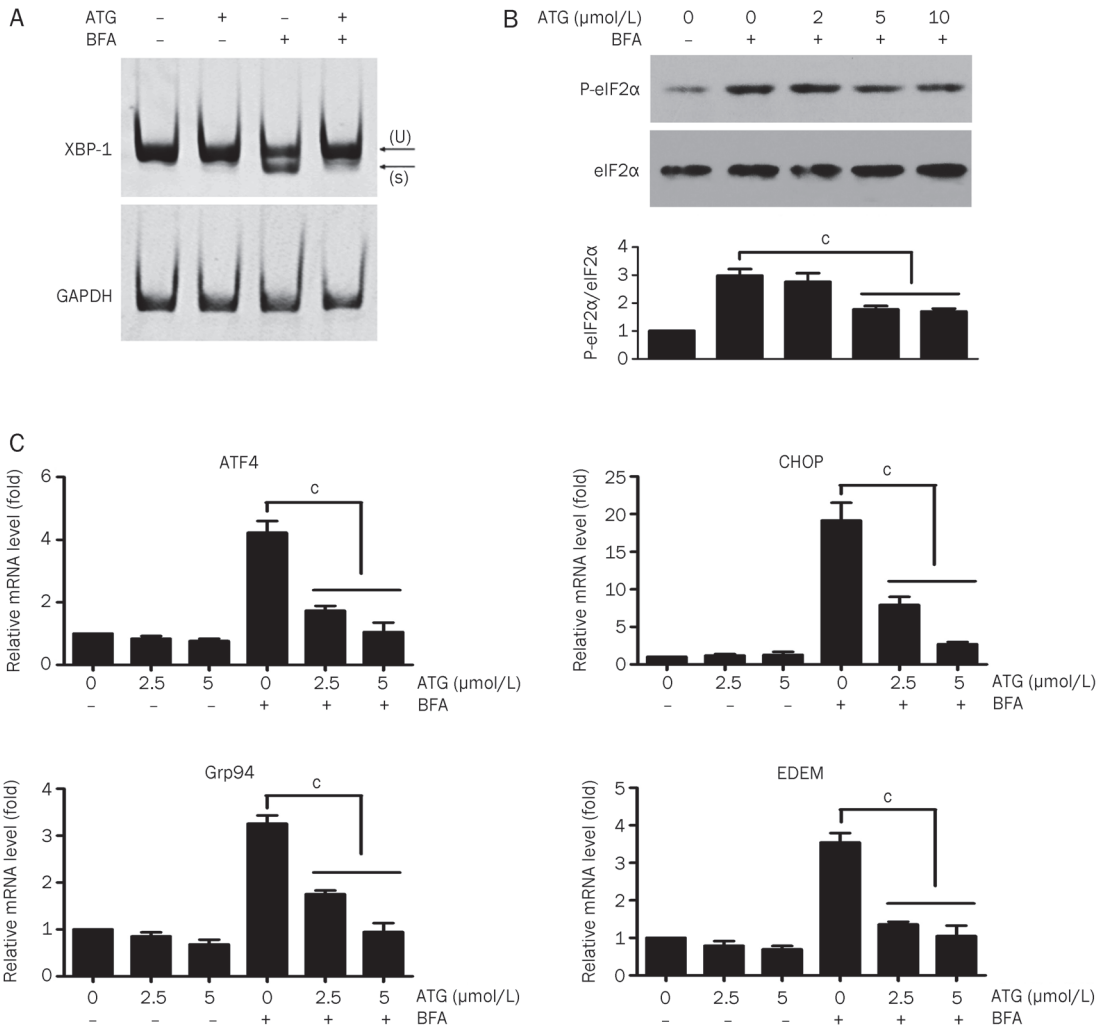

Figure 2. ATG significantly inhibits ER stress-induced UPR. (A) HepG2 cells were cultured for 6 h with or without ATG (5 μmol/L), in the presence or absence of BFA (100 nmol/L), and then lysed for RNA purification. Spliced (S) and unspliced forms of XBP1 mRNA (U) were detected using semi-quantitative RT-PCR. (B) HepG2 cells were cultured with the indicated concentrations of ATG for 3 h in the presence or absence of BFA (100 nmol/L) followed by cell lysis. The phosphorylation level of eIF2α at Ser51 was examined by Western blot analysis. Total eIF2α served as a loading control. The quantification of Western blot images of the ratio between P-eIF2α and eIF2α was shown in the lower panel. (C) HepG2 cells were treated with 0, 2.5, or 5 μmol/L ATG for 6 h, in the presence or absence of BFA (100 nmol/L). The expression levels of UPR downstream genes (Grp94, EDEM, ATF4 and CHOP) were examined by quantitative RT-PCR. n=3 experiments. Mean±SEM. $^cP<0.01$ *vs* control.

splicing form of XBP-1 mRNA (Figure 2A) as well as phosphorylation of eIF2α on serine (Ser) 51 (Figure 2B), which are two key events in the UPR. And ATG significantly inhibited the BFA-induced splicing of XBP-1 pre-mRNA and phosphorylation of eIF2α (Figure 2A and 2B).

We further used quantitative PCR to evaluate the effects of ATG on the expression of the downstream genes involved in the UPR, which include the activating transcription factor 4 (ATF4), the C/EBP homologous protein (CHOP), the glucose-regulated protein 94 (Grp94), and the ER degradation-enhancing alpha-mannosidase-like protein 1 (EDEM). Our data showed that ATG significantly inhibited BFA-induced expression of all four genes (Figure 2C). In addition, we also investigated the effect of ATG on the UPR induced by tunicamycin (TM), another ER stress inducer that inhibits N-linked glycosylation in the ER. As shown in supplymentary Figure 1, ATG significantly inhibited tunicamycin-induced splicing of XBP-1 pre-mRNA and mRNA expression of four downstream genes involved in the UPR. These results demonstrate that ATG protects cells from BFA-induced apoptosis via alleviating ER stress, and suggest that ATG may act upstream of the UPR, since all downstream signaling pathways were affected.

ATG attenuates protein translation

In mammalian cells, global translation attenuation is the first response to ER stress and is thought to be an important adaptive response that helps cells survive ER stress. Previous studies also reported that protein synthesis inhibitors such as cycloheximide[19] and salubrinal[20] displayed potential ER stress-relieving effects. Therefore, inhibition of protein syn-

thesis which reduces the load of substrates presented to the folding machinery in the ER lumen represents an important mechanism to alleviate ER stress[21]. To explore whether ATG affects protein synthesis, we transfected HepG2 cells with a plasmid encoding green fluorescent protein (GFP), and evaluated the effect of ATG on GFP expression by dividing the IOD (integral optical density) value of green fluorescence by the number of cells that was measured by Hoechst staining. As shown in Figure 3A, 24 h after treatment with ATG, the level of GFP protein was decreased in a dose-dependent manner. Cycloheximide (CHX) served as a positive control. However, neither artigenin nor CHX had effects on the mRNA level of GFP (Figure 3B). These data indicate that ATG can inhibit protein synthesis, which in turn reduces the load on the ER and thereby relieves ER stress.

To investigate how ATG regulates protein translation, we analyzed the effects of ATG on signaling proteins that are responsible for translational control, which include eIF2α, mTOR (the mammalian target of rapamycin) and p70S6K (p70 ribosomal protein S6 kinase), two components in mTOR signaling, and eEF2 (the eukaryotic translation elongation factor 2). Our data showed that ATG had no effects on the phosphorylation of eIF2α. However, it significantly inhibited the phosphorylation of mTOR and p70S6K in a dose dependent manner, and increased the phosphorylation/inactivation of eEF2 at threonine (Thr) 56 (Figure 3C).

We also examined the effects of ATG on these proteins in BFA-treated cells. BFA induced an increase in eIF2α phosphorylation, which was inhibited by ATG (Figure 3D), although ATG alone had no effect on the basal level phosphorylation of eIF2α. BFA had no effects on the phophorylation of either p70S6K or eEF2 (Figure 3D), suggesting that the inhibitory effect of ATG on protein translation was unaffected by BFA.

These data suggest that ATG attenuates protein synthesis likely through inhibiting mTOR-p70S6K signaling and eEF2 activity.

ATG reduces the unfolded protein response by activating AMPK

It has been reported that AMPK acts upstream of mTOR signaling and eEF2 in controlling translation. AMPK modulates the activity of mTOR either by direct phosphorylation and inhibition of mTOR[22], or by phosphorylation and activation of the tuberous sclerosis complex (TSC), an upstream regulator and inhibitor of mTOR activity[23]. The most characterized downstream effectors of mTOR are p70S6K and the eukaryotic translation initiation factor 4E (eIF4E)-binding protein 1 (4E-BP1), through which mTOR stimulates the initiation step of translation[24]. AMPK can also activate eEF2 kinase (eEF2K) either by direct phosphorylation of eEF2K at Ser398[25], or by inhibition of p70S6K. which phosphorylates and inactivates eEF2K at Ser366[26]. Activated eEF2K in turn phosphorylates and inactivates eEF2 at Thr56[27]. We therefore investigated the effect of ATG on AMPK phosphorylation/activation. As shown in Figure 4, ATG significantly stimulated the phosphorylation of AMPK at Thr172 of α catalytic subunit in a time- and dose-dependent manner (Figure 4A and 4B). ATG also increased the phosphorylation of ACC (acetyl-CoA carboxylase) at Ser79, a direct substrate of AMPK[28], indicating an increase in AMPK activity was induced (Figure 4B).

To determine whether the attenuation of protein translation by ATG is mediated by AMPK activation, we employed RNA interference to knock down AMPKα1. As shown in Figure 4C, siRNA-mediated AMPKα1 down-regulation partially reversed the effect of ATG on the phosphorylation of p70S6K and eEF2. These data suggest that AMPK activation at least partially mediates the inhibitory effect of ATG on protein translation.

To further verify that the alleviation of ER stress by ATG is mediated by AMPK activation, we used a selective inhibitor of AMPK, compound C (CC), to block AMPK activity. As shown in Figure 4D and 4E, compound CC significantly reduced the effects of ATG on the BFA-induced XBP-1 splicing and mRNA expression of Grp94, suggesting that the activation of AMPK is necessary for ATG's inhibitory effect on the BFA-induced UPR. Meanwhile, CC itself had no effects on the splicing of XBP-1 pre-mRNA (Figure 4D). The involvement of AMPK in the ATG inhibition of ER stress was further confirmed by using a known AMPK activator AICAR. Similar to artigenin, AICAR significantly prevented BFA-induced cell death in a dose-dependent manner (Figure 4F).

Taken together, our observations demonstrate that ATG alleviates ER stress probably through activating AMPK, which attenuates protein translation and reduces ER load.

ATG inhibits mitochondrial respiration, leading to AMPK activation

There are two main protein kinases involved in phosphorylating AMPK *in vivo*, LKB1 (liver kinase B1) and Ca^{2+}/calmodulin-denpendent protein kinase kinase, especially the β isoform (CaMKKβ)[29]. To determine whether the two kinases are critically involved in the ATG-induced AMPK phosphorylation, we used RNA interference to down-regulate the expression of LKB1 and CaMKKβ. As shown in Figure 5, knockdown of either LKB1 or CaMKKβ significantly reduced the phosphorylation of AMPK induced by ATG, suggesting that both kinases are involved in mediating the ATG-induced AMPK activation (Figure 5A).

Phosphorylation of AMPK by the two kinases is regulated by adenosine monophosphate (AMP), which allosterically activates AMPK and makes it a better substrate for the two upstream kinases and a poorer substrate for protein phosphatases[30]. The intracellular AMP level, however, is regulated by adenosine triphosphate (ATP) content. ATP depletion has been shown to increase AMP production as a consequence of the reaction catalyzed by adenylate kinase[30]. To investigate whether ATG affects ATP production, we evaluated intracellular ATP levels by a luciferase assay. As shown in Figure 5, intracellular ATP levels were reduced by ATG in a time-dependent and dose-dependent manner (Figure 5B and 5C).

Given the fact that mitochondria are the major ATP production organelles in eukaryotes, we investigated the effects of ATG on mitochondrial respiration in mitochondria isolated from rat muscle. Our data showed that ATG inhibited oxygen

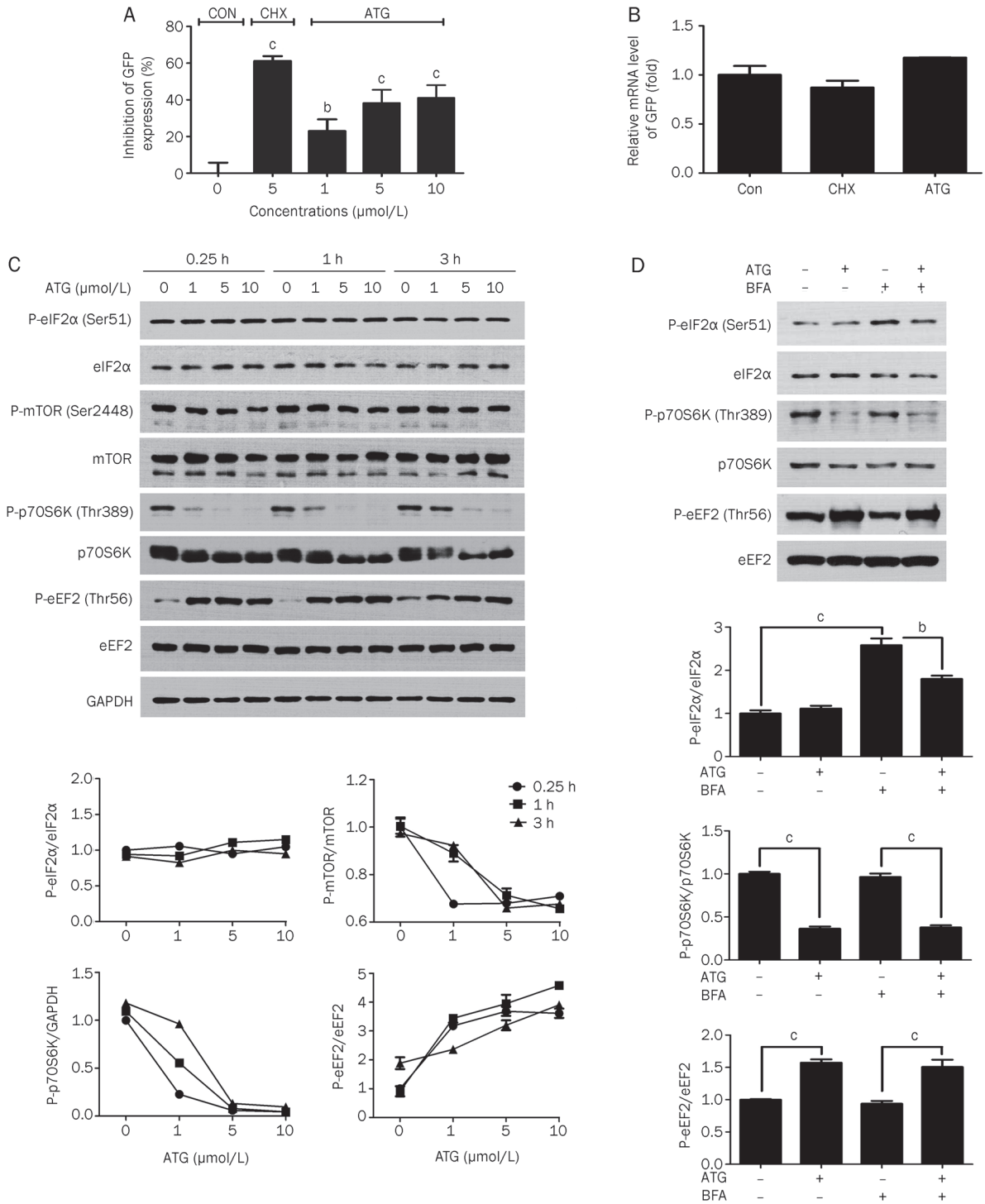

Figure 3. ATG moderately inhibits protein translation. (A) HepG2 cells were transfected with a GFP-expressing plasmid for 16 h, and then treated for another 24 h with DMSO, CHX (5 μmol/L), or the indicated concentrations of ATG followed by staining with Hoechst 33342 (2 μg/mL) for 5 min. At least six photographs per well in different areas of cell cultures were taken by fluorescence microscopy, and GFP expression was evaluated by dividing the IOD of green fluorescence by cell number. The value of GFP expression treated with DMSO was considered as 100%. (B) The expression levels of GFP mRNA were examined by quantitative RT-PCR. (C) HepG2 cells were treated for the indicated times with different concentrations of ATG. The phosphorylation levels of eIF2α, mTOR, p70S6K, and eEF2 were examined by Western blot analysis. Relative band intensity was expressed as a percentage compared with the value of control at 0.25 h. (D) HepG2 cells were cultured for 3 h in the presence or absence of ATG (5 μmol/L) and/or BFA (100 nmol/L) followed by cell lysis. The phosphorylation levels of eIF2α at Ser51, p70S6K at Thr389, and eEF2 at Thr56 were examined by Western blot analysis. Relative band intensity was expressed as a percentage compared with the value of untreated control. *n*=4 experiments. Mean±SEM. $^{b}P<0.05$, $^{c}P<0.01$ *vs* control.

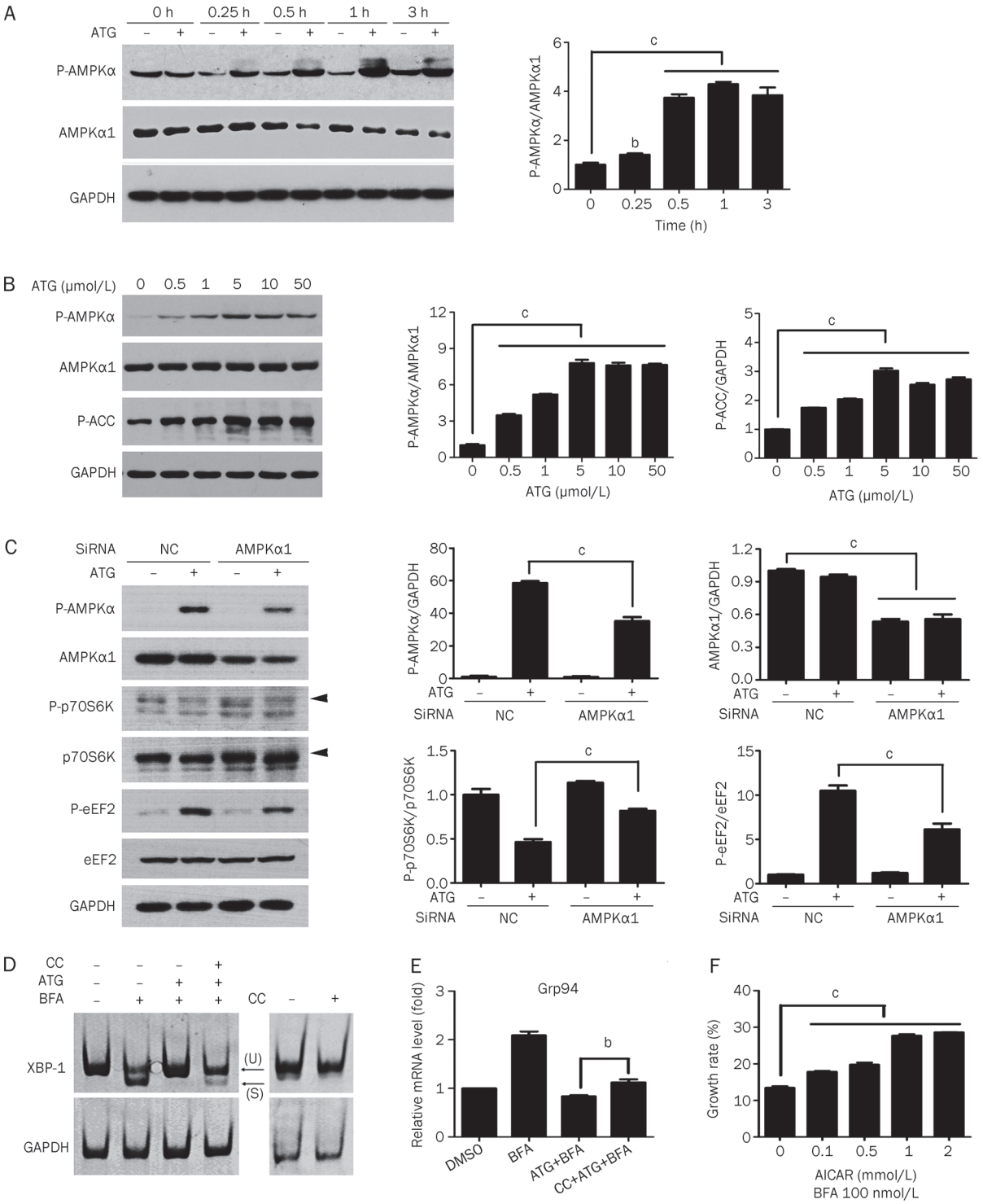

Figure 4. ATG activates AMPK and may lead to ER stress alleviation. (A and B) HepG2 cells were incubated with 5 μmol/L ATG for the indicated time (A) or with ATG at the indicated concentrations for 1 h (B). Phospho-AMPKα (Thr172), AMPKα1, and phospho-ACC (Ser79) were analyzed by Western blotting. GAPDH served as a control. Relative band intensity of each protein was expressed as a percentage compared with the value of untreated control. (C) HepG2 cells were transfected with a negative control siRNA (NC) or a siRNA targeting AMPKα1. At 48 h after transfection, cells were treated with or without ATG (5 μmol/L) for 1 h. Phospho-AMPKα (Thr172), AMPKα1, phospho-p70S6K (Thr389, indicated by an arrowhead), p70S6K (indicated by an arrowhead), phospho-eEF2 (Thr56), eEF2, and GAPDH were examined by Western blot analysis. The relative intensity of corresponding protein expression was shown in the right figures. (D and E) Pretreated with DMSO or CC (25 μmol/L) for 1 h, HepG2 cells were exposed to ATG (5 μmol/L) and/or BFA (100 nmol/L) for 6 h. Splicing of XBP1 mRNA was detected by semi-quantitative RT-PCR (D). mRNA expression of Grp94 was detected by quantitative RT-PCR (E). (F) HepG2 cells were treated with increasing concentrations of AICAR and 100 nmol/L BFA for 72 h. Cell growth rate was evaluated by MTT assay. n=4 experiments. Mean±SEM. $^{b}P<0.01$, $^{c}P<0.01$ *vs* control.

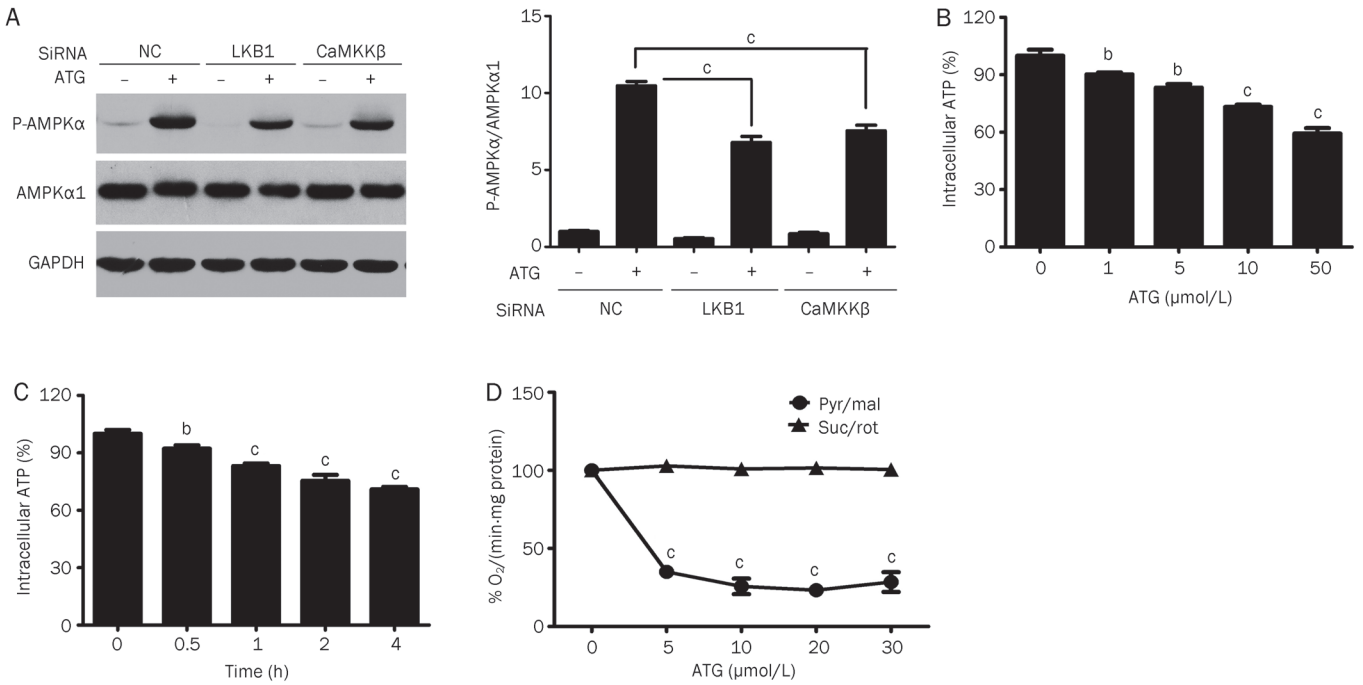

Figure 5. ATG inhibits mitochondrial respiration. (A) HepG2 cells were transfected with a negative control siRNA (NC) or siRNA targeting LKB1 or CaMKKβ. After 48 h of transfection, cells were treated with or without ATG (5 μmol/L) for 1 h. Phospho-AMPKα (Thr172) and AMPKα1 were examined by Western blot analysis. Relative band intensity was expressed as a percentage compared with the value of untreated control. (B and C) Intracellular ATP levels were measured by the luciferin-luciferase method. HepG2 cells were incubated with various concentrations of ATG for 1 h (B) or with 5 μmol/L ATG for the indicated periods of time (C). (D) Oxygen consumption rates were measured in mitochondria at 37 °C using substrates combinations targeting respiratory complex I (5 mmol/L pyruvate plus 2 mmol/L malate) or complex II (10 mmol/L succinate plus 4 μmol/L rotenone). n=4 experiments. Mean±SEM. $^bP<0.05$, $^cP<0.01$ *vs* control.

consumption in a dose-dependent manner in the presence of substrates for complex I (pyruvate plus malate). In contrast, no effect of ATG on mitochondrial respiration was observed in the presence of substrate for complex II (succinate) and rotenone (Figure 5D).

Taken together, our data demonstrate that ATG selectively inhibits mitochondrial respiration supported by substrates for complex I and decreases ATP production likely leading to AMPK phosphorylation/activation.

ATG protects INS-1 β-cells from palmitate-induced cell death

It has been reported that exposure to high concentrations of free (nonesterified) fatty acid (FFA) induces ER stress and causes β-cell apoptosis[8, 31], which has been considered as one of the major causes of insufficient insulin production in type 2 diabetes[32, 33]. We therefore investigated the effects of ATG on palmitate-induced β-cell death. Palmitate severely decreased cell viability of INS-1 β-cells, while treatment with ATG significantly prevented cell death in a dose-dependent manner (Figure 6A). We then investigated whether ATG could activate AMPK in INS-1 cells. Our data showed that ATG significantly increased the phosphorylation of AMPK in the absence or presence of palmitate (Figure 6B). Furthermore, we examined the effects of ATG on palmitate-induced UPR in INS-1 cells. As shown in Figure 6C, 6D, and 6E, palmitate promoted the splicing of XBP-1 pre-mRNA and the mRNA expression of Grp78 and Grp94, which were significantly inhibited by ATG. These data suggest that ATG protects INS-1 cells from palmitate-induced cell death probably through alleviating ER stress and the protective effects of ATG against ER stress are not specific in HepG2 cells.

Discussion

There has been growing interest in therapeutic strategies to alleviate ER stress, since prolonged ER stress has been associated with a wide range of pathological conditions[5]. ER stress has been thought to play a central role in the pathogenesis of type 2 diabetes not only because of its role in the induction of insulin resistance but also because of its involvement in β-cell death, a common feature of type 2 diabetes[34]. Therefore, compounds that alleviate ER stress may act as therapeutic agents for the treatment of β-cell loss in type 2 diabetes. In this study, we have identified ATG, a natural product from *Arctium lappa* L, as a candidate for alleviating ER stress.

Firstly, we presented two lines of evidences to demonstrate that ATG was an ER stress alleviator (Figure 1, 2, and supplementary Figure 1). First, ATG protected HepG2 cells from ER stress inducer BFA-induced apoptosis, but showed no protective effect against non-ER stress stimuli. Our data showed that the lowest effective dose of ATG is 2.5 μmol/L and ATG at

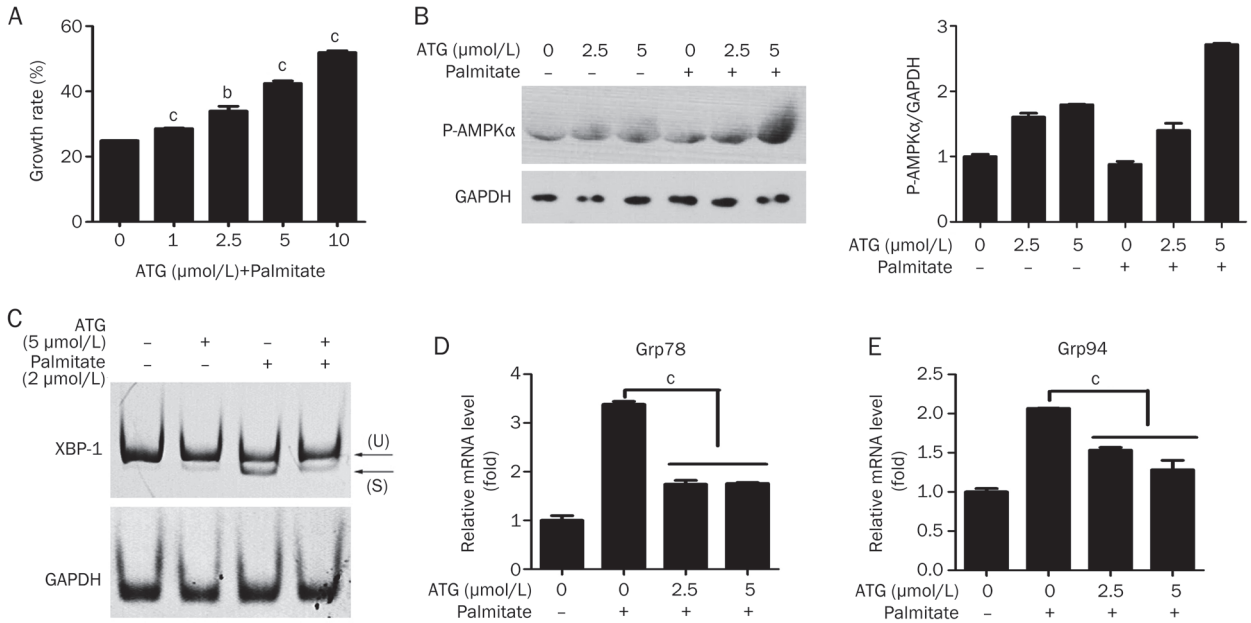

Figure 6. ATG prevents palmitate-induced cell death and ER stress in INS-1 β-cells. (A) INS-1 β-cells were incubated with the indicated concentrations of ATG in the presence of palmitate (2 mmol/L) for 24 h. Cell growth rate was evaluated by MTT assay. (B) INS-1 cells were treated with the indicated concentrations of ATG in the presence and absence of palmitate for 3 h. Phospho-AMPKα (Thr172) and GAPDH were analyzed by Western blotting. The quantification of Western blot images of the ratio between P-AMPKα and GAPDH was shown in the right panel. (C, D, and E) INS-1 cells were incubated with the indicated concentrations of ATG and palmitate for 6 h, followed by RNA purification and reverse transcription. Splicing of XBP1 mRNA in INS-1 β-cell was detected by semi-quantitative RT-PCR (C). mRNA expressions of Grp78 (D) and Grp94 (E) were detected by quantitative RT-PCR. n=4. Mean±SEM. $^{b}P<0.05$, $^{c}P<0.01$ *vs* control.

higher dose (>10 μmol/L) displayed cytotoxicity, which might suggest a narrow therapeutic window. However, our data also showed that the protective effect of ATG at 10 μmol/L was quite marked. We therefore assume that ATG may have a wider therapeutic range in clinical settings. Second, ATG inhibited BFA- and tunicamycin-induced UPR, *ie*, the splicing of XBP-1 pre-mRNA, the phosphorylation of eIF2α and the expression of downstream UPR target genes, including Grp94, EDEM, ATF4, and CHOP. The UPR is involved in both survival and the apoptotic response[35]. Whether a cell survives or dies upon ER stress will depend on the balance of these opposing signals. In this case, BFA-induced ER stress caused cell apoptosis, which means that the pro-death signal overrides the pro-survival signal. Inhibition of the UPR by ATG promoted cell survival, although ATG inhibited both pro-survival and pro-death signaling downstream of the UPR.

To investigate whether ATG alleviates ER stress through attenuating protein synthesis, we analyzed the effects of ATG on the protein expression level of a transfected GFP gene. Our data demonstrated that ATG decreased the level of GFP protein without influencing its transcription (Figure 3A and 3B). We also examined the effects of ATG on protein degradation and autophagy. Our data showed that ATG had no effects on either protein degradation or autophagy (unpublished data). We therefore conclude that ATG reduced protein expression level by inhibiting protein translation but not transcription or degradation, by which ATG may relieve ER stress.

Unlike some of the ER stress alleviators, such as salubrinal which reduces ER load by inducing the phosphorylation of eIF2α[20], therefore inhibiting the initiation of protein translation, ATG did not seem to affect the initiation factor eIF2α, but significantly inhibited phosphorylation of mTOR-p70S6K signaling and induced phosphorylation/inactivation of the protein translation elongation factor eEF2 (Figure 3C and 3D), suggesting that ATG attenuates protein synthesis by inhibiting both translation initiation and elongation.

Therefore, inhibition of protein synthesis represents an effective strategy to reduce ER stress. Once the protein synthesis is reduced, inhibition of downstream protein modification and/or folding, as caused by BFA and/or TM, will no longer elicit an UPR. Consistent with this notion, the BFA-induced phosphorylation of eIF2α is inhibited by ATG, although ATG itself does not directly affect eIF2α phosphorylation (Figure 3D).

Both mTOR-p70S6K signaling and eEF2 have been reported to be regulated by AMPK[36]. We therefore investigated whether ATG activated AMPK, and if so, whether AMPK activation mediated ATG action. Our data showed that ATG obviously increased the phosphorylation/activation of AMPK. Encouragingly, knockdown of AMPKα1 by RNA interference partially reversed the effect of ATG on the phosphorylation of p70S6K and eEF2. Furthermore, an AMPK inhibitor, compound C, could block the inhibitory effect of ATG on BFA-induced XBP-1 splicing, whereas an AMPK activator, AICAR, could mimic ATG to reduce the ER stress-induced cell death.

These data strongly suggest that AMPK plays a central role in mediating all of the ATG effects in alleviating ER stress. Our results, together with an earlier report[37], also indicate that activating AMPK could be an effective strategy for ER stress reduction.

AMPK is widely recognized as a key regulator of fatty acid and glucose homeostasis[30], and the activation of AMPK has been considered an attractive strategy for the treatment of type 2 diabetes. The most representative compounds are metformin and berberine, which exert anti-diabetic effects through activating AMPK[18, 38]. Meanwhile, they are also reported to possess protective effect against ER stress[39–41]. Given the crucial role of ER stress in the development of pancreatic β-cell loss and insulin resistance in type 2 diabetes[6], the alleviation of ER stress by AMPK may play an important role in treating type 2 diabetes. Consistent with this notion, our data demonstrated that ATG also protected INS-1 β-cells against palmitate-induced ER stress and cell death (Figure 6). In addition, activating AMPK may also represent a potential therapeutic strategy to relieve ER stress in other ER stress-related diseases, since ER stress is associated with a number of diseases.

AMPK has been reported to be activated by its two main upstream kinases, LKB1 and CaMKKβ in response to decreased intracellular levels of ATP[29]. Our data showed that AMPK phosphorylation induced by ATG was significantly inhibited by either LKB1 or CaMKKβ siRNAs, implying that both kinases are involved in ATG-induced AMPK phosphorylation (Figure 5A). This is consistent with a recent study that reported ATG phosphorylated AMPK in H9C2 and C2C12 cells via LKB1 and CaMKK-denpendent pathways[42]. Furthermore, we found the intracellular ATP level was significantly reduced by ATG (Figure 5B and 5C), which might also lead to AMPK activation. Interestingly, ATG at 0.5 μmol/L and 1 μmol/L significantly increased AMPK phosphorylation but slightly reduced the intracellular ATP levels, which implies that ATG may also activate AMPK via an ATP depletion-independent manner. Taken together, our data suggest that ATG activates AMPK probably through activating LKB1 and CaMKKβ and/or decreasing the ATP level.

Since oxidative phosphorylation and glycolysis are the two main sources of ATP in eukaryotic cells, we then investigated the effects of ATG on mitochondrial respiratory function. Our data demonstrated that ATG inhibited oxygen consumption supported by substrates for complex I but not that supported by complex II substrates (Figure 5D), indicating that the inhibition of mitochondrial respiration by ATG was occurring either at the level of NADH production or at complex I. These results suggest that ATG decreases the intracellular level of ATP and increases the phosphorylation/activity of AMPK through inhibiting mitochondrial respiration.

In conclusion, our findings reveal the molecular mechanism by which ATG alleviates ER stress: the inhibition of mitochondrial respiration by ATG results in reduced ATP production in mitochondria. Under conditions of energy depletion, AMPK is probably activated by LKB1 and CaMKKβ, which in turn inhibits mTOR-p70S6K signaling and increases eEF2 phosphorylation/inactivation, leading to the attenuation of protein synthesis. As a result, the burden of ER stress is relieved, and cell death is prevented (Figure 7). We also show the protective effect of ATG against palmitate-induced INS-1 β-cell death. These data suggest that ATG may represent a potential therapeutic intervention for treating ER stress-related diseases, such as β-cell loss in type 2 diabetes.

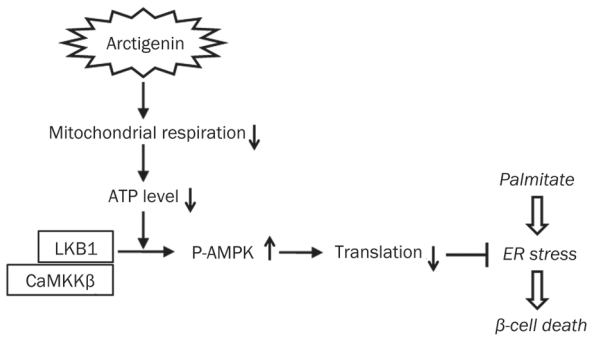

Figure 7. A schematic model of the mechanism of ATG action. ATG inhibits mitochondrial respiration resulting in a reduction in ATP level and an activation of AMPK. Activated AMPK attenuates protein translation, leading to a reduction of the load on the ER and an alleviation of ER stress. As a result, ATG protects INS-1 β-cells from palmitate-induced cell death.

Acknowledgements

This work was supported by the National Science & Technology Major Project "Key New Drug Creation and Manufacturing Program", China (Number: 2009ZX09301-001 and 2009ZX09103-064); the China Ministry of Science and Technology Research Grant 2008ZX10002-020; and the Shanghai Science and Technology Research Grants 08DZ1971403 and 09JC1416700.

Author contribution

Yuan GU, Jun-ying YUAN, and Qiang YU participated in research design; Yuan GU, Xiao-xiao SUN, Ji-ming YE, and Li HE conducted experiments; Shou-sheng YAN, Hao-hao ZHANG, and Li-hong HU contributed to essential reagents or analytic tools; Yuan GU and Qiang YU performed data analysis; Yuan GU and Qiang YU wrote the manuscript.

Supplementary information

Supplementary figures are available at website of Acta Pharmacologica Sinica on NPG.

References

1 Sood R, Porter AC, Ma K, Quilliam LA, Wek RC. Pancreatic eukaryotic initiation factor-2alpha kinase (PEK) homologues in humans, *Drosophila melanogaster* and *Caenorhabditis elegans* that mediate translational control in response to endoplasmic reticulum stress. Biochem J 2000; 346: 281–93.

2 Shen J, Chen X, Hendershot L, Prywes R. ER stress regulation of ATF6 localization by dissociation of BiP/GRP78 binding and unmasking of Golgi localization signals. Dev Cell 2002; 3: 99–111.

3 Yoshida H, Matsui T, Yamamoto A, Okada T, Mori K. XBP1 mRNA is induced by ATF6 and spliced by IRE1 in response to ER stress to produce a highly active transcription factor. Cell 2001; 107: 881–91.
4 Ron D, Walter P. Signal integration in the endoplasmic reticulum unfolded protein response. Nat Rev Mol Cell Biol 2007; 8: 519–29.
5 Kim I, Xu W, Reed JC. Cell death and endoplasmic reticulum stress: disease relevance and therapeutic opportunities. Nat Rev Drug Discov 2008; 7: 1013–30.
6 Eizirik DL, Cardozo AK, Cnop M. The role for endoplasmic reticulum stress in diabetes mellitus. Endocr Rev 2008; 29: 42–61.
7 Ozcan U, Cao Q, Yilmaz E, Lee AH, Iwakoshi NN, Ozdelen E*, et al.* Endoplasmic reticulum stress links obesity, insulin action, and type 2 diabetes. Science 2004; 306: 457–61.
8 Laybutt DR, Preston AM, Akerfeldt MC, Kench JG, Busch AK, Biankin AV*, et al.* Endoplasmic reticulum stress contributes to beta cell apoptosis in type 2 diabetes. Diabetologia 2007; 50: 752–63.
9 Cho MK, Jang YP, Kim YC, Kim SG. Arctigenin, a phenylpropanoid dibenzylbutyrolactone lignan, inhibits MAP kinases and AP-1 activation via potent MKK inhibition: the role in TNF-alpha inhibition. Int Immunopharmacol 2004; 4: 1419–29.
10 Zhao F, Wang L, Liu K. *In vitro* anti-inflammatory effects of arctigenin, a lignan from *Arctium lappa* L, through inhibition on iNOS pathway. J Ethnopharmacol 2009; 122: 457–62.
11 Chan YS, Cheng LN, Wu JH, Chan E, Kwan YW, Lee SM*, et al.* A review of the pharmacological effects of *Arctium lappa* (burdock). Inflammopharmacology 2011; 19: 245–54.
12 Cervellati R, Speroni E, Govoni P, Guerra MC, Costa S, Arnold UW*, et al. Wulfenia carinthiaca* Jacq., antioxidant and pharmacological activities. Z Naturforsch C 2004; 59: 255–62.
13 Charlton JL. Antiviral activity of lignans. J Nat Prod 1998; 61: 1447–51.
14 Awale S, Lu J, Kalauni SK, Kurashima Y, Tezuka Y, Kadota S*, et al.* Identification of arctigenin as an antitumor agent having the ability to eliminate the tolerance of cancer cells to nutrient starvation. Cancer Res 2006; 66: 1751–7.
15 Sun S, Wang X, Wang C, Nawaz A, Wei W, Li J*, et al.* Arctigenin suppresses unfolded protein response and sensitizes glucose deprivation-mediated cytotoxicity of cancer cells. Planta Med 2011; 77: 141–5.
16 Kim JY, Hwang JH, Cha MR, Yoon MY, Son ES, Tomida A*, et al.* Arctigenin blocks the unfolded protein response and shows therapeutic antitumor activity. J Cell Physiol 2010; 224: 33–40.
17 Hayashi K, Narutaki K, Nagaoka Y, Hayashi T, Uesato S. Therapeutic effect of arctiin and arctigenin in immunocompetent and immunocompromised mice infected with influenza A virus. Biol Pharm Bull 2010; 33: 1199–205.
18 Turner N, Li JY, Gosby A, To SW, Cheng Z, Miyoshi H*, et al.* Berberine and its more biologically available derivative, dihydroberberine, inhibit mitochondrial respiratory complex I: a mechanism for the action of berberine to activate AMP-activated protein kinase and improve insulin action. Diabetes 2008; 57: 1414–8.
19 Bi M, Naczki C, Koritzinsky M, Fels D, Blais J, Hu N*, et al.* ER stress-regulated translation increases tolerance to extreme hypoxia and promotes tumor growth. EMBO J 2005; 24: 3470–81.
20 Boyce M, Bryant KF, Jousse C, Long K, Harding HP, Scheuner D*, et al.* A selective inhibitor of eIF2alpha dephosphorylation protects cells from ER stress. Science 2005; 307: 935–9.
21 Ron D. Translational control in the endoplasmic reticulum stress response. J Clin Invest 2002; 110: 1383–8.
22 Cheng SW, Fryer LG, Carling D, Shepherd PR. Thr2446 is a novel mammalian target of rapamycin (mTOR) phosphorylation site regulated by nutrient status. J Biol Chem 2004; 279: 15719–22.
23 Inoki K, Zhu T, Guan KL. TSC2 mediates cellular energy response to control cell growth and survival. Cell 2003; 115: 577–90.
24 Mamane Y, Petroulakis E, LeBacquer O, Sonenberg N. mTOR, translation initiation and cancer. Oncogene 2006; 25: 6416–22.
25 Browne GJ, Finn SG, Proud CG. Stimulation of the AMP-activated protein kinase leads to activation of eukaryotic elongation factor 2 kinase and to its phosphorylation at a novel site, serine 398. J Biol Chem 2004; 279: 12220–31.
26 Wang X, Li W, Williams M, Terada N, Alessi DR, Proud CG. Regulation of elongation factor 2 kinase by p90 (RSK1) and p70 S6 kinase. EMBO J 2001; 20: 4370–9.
27 Redpath NT, Price NT, Severinov KV, Proud CG. Regulation of elongation factor-2 by multisite phosphorylation. Eur J Biochem 1993; 213: 689–99.
28 Carlson CA, Kim KH. Regulation of hepatic acetyl coenzyme A carboxylase by phosphorylation and dephosphorylation. J Biol Chem 1973; 248: 378–80.
29 Hardie DG. The AMP-activated protein kinase pathway--new players upstream and downstream. J Cell Sci 2004; 117: 5479–87.
30 Hardie DG. Minireview: the AMP-activated protein kinase cascade: the key sensor of cellular energy status. Endocrinology 2003; 144: 5179–83.
31 Elouil H, Bensellam M, Guiot Y, Vander Mierde D, Pascal SM, Schuit FC*, et al.* Acute nutrient regulation of the unfolded protein response and integrated stress response in cultured rat pancreatic islets. Diabetologia 2007; 50: 1442–52.
32 Pick A, Clark J, Kubstrup C, Levisetti M, Pugh W, Bonner-Weir S*, et al.* Role of apoptosis in failure of beta-cell mass compensation for insulin resistance and beta-cell defects in the male Zucker diabetic fatty rat. Diabetes 1998; 47: 358–64.
33 Bonner-Weir S. Islet growth and development in the adult. J Mol Endocrinol 2000; 24: 297–302.
34 Cnop M. Fatty acids and glucolipotoxicity in the pathogenesis of type 2 diabetes. Biochem Soc Trans 2008; 36: 348–52.
35 Kitamura M. Endoplasmic reticulum stress and unfolded protein response in renal pathophysiology: Janus faces. Am J Physiol Renal Physiol 2008; 295: F323–34.
36 Chan AY, Dyck JR. Activation of AMP-activated protein kinase (AMPK) inhibits protein synthesis: a potential strategy to prevent the development of cardiac hypertrophy. Can J Physiol Pharmacol 2005; 83: 24–8.
37 Terai K, Hiramoto Y, Masaki M, Sugiyama S, Kuroda T, Hori M*, et al.* AMP-activated protein kinase protects cardiomyocytes against hypoxic injury through attenuation of endoplasmic reticulum stress. Mol Cell Biol 2005; 25: 9554–75.
38 Musi N, Hirshman MF, Nygren J, Svanfeldt M, Bavenholm P, Rooyackers O*, et al.* Metformin increases AMP-activated protein kinase activity in skeletal muscle of subjects with type 2 diabetes. Diabetes 2002; 51: 2074–81.
39 Kim DS, Jeong SK, Kim HR, Chae SW, Chae HJ. Metformin regulates palmitate-induced apoptosis and ER stress response in HepG2 liver cells. Immunopharmacol Immunotoxicol 2010; 32: 251–7.
40 Hao X, Yao A, Gong J, Zhu W, Li N, Li J. Berberine ameliorates pro-inflammatory cytokine-induced endoplasmic reticulum stress in human intestinal epithelial cells *in vitro*. Inflammation 2012; 35: 841–9.
41 Wang ZS, Lu FE, Xu LJ, Dong H. Berberine reduces endoplasmic reticulum stress and improves insulin signal transduction in Hep G2 cells. Acta Pharmacol Sin 2010; 31: 578–84.
42 Tang X, Zhuang J, Chen J, Yu L, Hu L, Jiang H*, et al.* Arctigenin efficiently enhanced sedentary mice treadmill endurance. PLoS One 2011; 6: e24224.